

COMPUTATIONAL PHYSICS

The Computational Physics Section publishes articles that help students and their instructors learn about the physics and the computational tools used in contemporary research. Most articles will be solicited, but interested authors should email a proposal to the editors of the Section, Jan Tobochnik (jant@kzoo.edu) or Harvey Gould (hgould@clarku.edu). Summarize the physics and the algorithm you wish to include in your submission and how the material would be accessible to advanced undergraduates or beginning graduate students.

The hardwall method of solving the radial Schrödinger equation and unmasking hidden symmetries

Siu A. Chin^{a)} and John Massey^{b)}

Department of Physics and Astronomy, Texas A&M University, College Station, Texas 77843-4242

(Received 30 January 2019; accepted 18 May 2019)

Solving for the bound state eigenvalues of the Schrödinger equation is a tedious iterative process using the conventional shooting or matching method. In this paper, we bypass a eigenvalue's dependence on the eigenfunction by trying all eigenvalues to a desired accuracy. When the eigenvalue is known, the integration for the eigenfunction is then trivial. By outputting the radial distance at which the wave function crosses zero (the hardwall radius) for a given energy, the hardwall method automatically determines the entire spectrum of eigenvalues of the radial Schrödinger equation without iterative adjustments. Moreover, such a spherically symmetric hardwall can unmask the accidental degeneracy of eigenvalues due to hidden symmetries. We illustrate the method for the Coulomb, harmonic, Coulomb plus harmonic, and the Woods-Saxon potentials. © 2019 American Association of Physics Teachers.

<https://doi.org/10.1119/1.5111839>

I. INTRODUCTION

Solving the radial Schrödinger equation for a central potential $V(r)$

$$-\frac{\hbar^2}{2m} \left(\frac{\partial^2}{\partial r^2} - \frac{\ell(\ell+1)}{r^2} \right) u(r) + V(r)u(r) = Eu(r), \quad (1)$$

where $u(r) = rR_{n\ell}(r)$, is an important teaching tool¹ and a standard subject in Koonin's early computational physics text.² In recent years, this topic is not discussed in most computational physics texts,³⁻⁷ or only alluded to briefly.⁵ Perhaps, this lack is related to the difficulty of implementing the conventional shooting or matching method^{1,3-7} of solving the eigenvalue problem. Although more sophisticated methods have been suggested,⁸⁻¹¹ we introduce here a classroom-tested, start-from-scratch method that might be the simplest among the known ways of solving the bound state problem of the radial Schrödinger equation.

Our simplification follows from two key ideas: the eigenvalue E is usually determined by requiring the eigenfunction to satisfy certain boundary conditions. The adjustment of the eigenvalue by shooting or matching the eigenfunction³⁻⁷ to satisfy the boundary condition is a tedious iterative process. In this work, we completely by-pass this adjustment process by sweeping through all values of E to a desired accuracy. That is, we simply try all values of E , up to a certain precision, by brute force. When E is known, the eigenfunction can be obtained easily. This procedure breaks the dependence of the eigenvalue on the eigenfunction.

To decide which E is the correct eigenvalue, we observe that every value of E is an eigenvalue of the given potential plus an infinite potential barrier at some radius C . The correct eigenvalue E is then obtained in the limit $C \rightarrow \infty$. Given E , C is the radial distance where the wave function vanishes. This “hardwall” condition will be described in Sec. III. Our method takes advantage of the fact that it is much easier to find C as a function of E , than the other way around, as in the matrix method.¹¹ Also in contrast to the matrix method, no basis functions need to be assumed, no matrix elements need to be computed, and no matrix needs to be diagonalized.

This brute-force approach is conceptually simple and can be easily understood by undergraduates taking a first course in quantum mechanics. By leveraging the power of modern computers, this approach can decipher the entire spectrum of a central potential automatically without piecemeal adjustments. Moreover, this method can unmask hidden symmetries by revealing the “accidental degeneracy” of eigenvalues and their patterns of degeneracy.

II. SOLVING THE RADIAL SCHRÖDINGER EQUATION NUMERICALLY

To numerically solve the reduced radial Schrödinger equation (1), we first cast it into an appropriate dimensionless form. This digression is appropriate because most texts³⁻⁷ do not emphasize this important point.

To arrive at a dimensionless equation, we first set $r = r^*a$, where a is a unit of length to be determined and r^* is dimensionless. Equation (1) then reads

$$-\frac{\hbar^2}{2ma^2} \left(\frac{\partial^2}{\partial r^{*2}} - \frac{\ell(\ell+1)}{r^{*2}} \right) u(r^*) + V(r^*a)u(r^*) = Eu(r^*). \quad (2)$$

Because $e_0 \equiv \hbar^2/ma^2$ is a unit of energy, it is natural to write $E = E^*e_0$ so that Eq. (1) has the dimensionless form

$$-\frac{1}{2} \left(\frac{\partial^2}{\partial r^{*2}} - \frac{\ell(\ell+1)}{r^{*2}} \right) u(r^*) + v(r^*)u(r^*) = E^*u(r^*), \quad (3)$$

where the dimensionless potential is given by

$$v(r^*) = \frac{V(r^*a)}{e_0} = \frac{ma^2V(r^*a)}{\hbar^2}. \quad (4)$$

We choose a so that $v(r^*)$ is as simple as possible. For example, for the Coulomb potential with $V(r) = -ke^2/r$, the dimensionless potential is

$$v(r^*) = -\frac{ma^2ke^2}{r^*a\hbar^2} = -\frac{1}{r^*}, \quad (5)$$

for the choice $a = \hbar^2/(mke^2)$, which is the Bohr radius. The unit of energy e_0 is then the Hartree (Ha), and the spectrum of the hydrogen atom is $E = -1/(2n^2)$ Ha. (Note that 1 Ha = 2 Ry (Rydberg) = 2(13.6 eV).) This choice defines the atomic units most appropriate for treating atomic problems. Another example is the harmonic potential, with $V(r) = (1/2)m\omega^2r^2$. In this case,

$$v(r^*) = \frac{ma^2m\omega^2a^2r^{*2}}{2\hbar^2} = \frac{1}{2}r^{*2}, \quad (6)$$

with the natural choice of $a = \sqrt{\hbar/m\omega}$, which is the harmonic length, and $e_0 = \hbar^2/ma^2 = \hbar\omega$.

The advantage of solving a dimensionless equation is that we solve an entire class of equations at once, not just one particular equation. For example, if we are interested in solving the Coulomb potential with a nuclear charge Ze , there is no need for a new calculation. We simply change the units from $k \rightarrow kZ$ and see immediately that the Bohr radius will shrink by a factor of Z and the energy increases by a factor of Z^2 . If we are interested in muonic atoms, where the electron is replaced by the muon which is 207 times more massive, then the radius of muonic hydrogen will be 207 times smaller with binding energy $(207)^2$ times greater. Similarly for the harmonic case, the dimensionless equation solves an entire class of problems with any values of m and ω . These important insights are lost when explicit units are used, as done in some computational texts.³

From this point forward, we will drop all asterisks in referencing the dimensionless radial equation (3).

The eigenvalue problem associated with the radial equation (3) is the determination of E subject to the boundary conditions $u(0)=0$ and $u(\infty)=0$. The shooting method starts out at $u(0)=0$, integrates out to some large value of $r=R$, and adjusts E so that $u(R)=0$. The needed R value is different for different eigenstates.

In this work, as in the shooting method, we will also start at the origin with $u(0)=0$ and integrate outward, but we will not need to impose the condition $u(R)=0$ for an *a priori* unknown R value. Instead, we will introduce the hardwall condition to be described in Sec. III.

The dimensionless radial equation (3) can be further arranged as

$$\frac{\partial^2 u(r)}{\partial r^2} = f(r)u(r), \quad (7)$$

where

$$f(r) = \frac{\ell(\ell+1)}{r^2} + 2V(r) - 2E. \quad (8)$$

It is well known that Eq. (7) can be solved efficiently by the fourth-order Numerov¹² algorithm^{1,2,13,14}

$$\begin{aligned} & \left(1 - \frac{1}{12}\Delta r^2 f_{j+1} \right) u_{j+1} \\ &= \left(2 + \frac{5}{6}\Delta r^2 f_j \right) u_j - \left(1 - \frac{1}{12}\Delta r^2 f_{j-1} \right) u_{j-1}, \end{aligned} \quad (9)$$

where $u_j = u(j\Delta r)$ and $f_j = f(j\Delta r)$. For a given Δr , we can define

$$g_j = 1 - \frac{1}{12}\Delta r^2 f_j \quad (10)$$

so that the algorithm reads simply

$$u_{j+1} = \frac{(12 - 10g_j)u_j - g_{j-1}u_{j-1}}{g_{j+1}}. \quad (11)$$

The Numerov algorithm in Eq. (11) is used to obtain all the results reported in this work.

III. THE HARDWALL CONDITION

The hardwall method replaces the $u(\infty)=0$ boundary condition with the hardwall condition: for a given set of ℓ and E values, $u(r)$ is iterated outward using Eq. (11) with a chosen value of Δr , with $u_0=0$ and u_1 an arbitrary but small real number, out to a large value of $r=R$, depending on the number of eigenvalues desired. Whenever u_j crosses zero, that is, $u_{j-1}u_j < 0$, we output (C, E) , where E is the given energy and $C = (j - 1/2)\Delta r$ is the hardwall radius. That is, whenever u_j crosses zero, E is the exact energy corresponding to the original potential $v(r)$ plus an infinite potential (the hardwall) at $r=C$. In other words, every value of E is an eigenvalue for $v(r)$ plus a hardwall potential for some value of C . For each value of ℓ , we do the same outward integration of u_j over a set of prescribed E values spanning the bound state range of $v(r)$. If E is plotted as a function of C after an interval of E has been swept, we will see that E converges to the eigenvalue of $v(r)$ for large C .

We first show how the hardwall method works for the null-potential case of $v(r)=0$. In this case, the solutions to the radial Schrödinger equation are spherical Bessel functions $j_\ell(k_{ln}r)$, with energy eigenvalues $E_{ln} = (1/2)k_{ln}^2$. For $\ell=0$, $j_0 = \sin(k_{0n}r)/k_{0n}r$. For an infinite wall at the hardwall radius C , the wave function must vanish, forcing $k_{0n}C = n\pi$ and $E = (1/2)(n\pi/C)^2$. We compare the output (C, E) of the hardwall method with this analytical result in Fig. 1. We shall refer to this (C, E) plot of the hardwall method as a “ C -scan” of the potential. For this calculation, we set $\ell=0$ and iterate over an outer loop of 50 values of

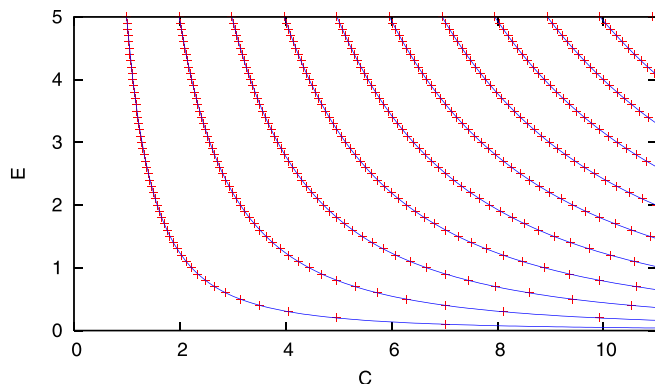


Fig. 1. Symbols are energy eigenvalues using the hardwall method for $v=0$. The first ten eigenvalues for $\ell=0$ are shown. Solid lines are the exact energies $E = (1/2)(n\pi/C)^2$ for $n=1-10$.

$E_i = i\Delta E$, with $\Delta E = 0.1$ and an inner loop of 1100 values of $r = j\Delta r$ with $\Delta r = 0.01$ out to $C = 11$ (so that only 10 eigenvalues are visible). This calculation demonstrates the essential characteristic of the method:

- (1) At any fixed value of C , the C -scan gives the correct eigenvalues of the hardwall potential at $r=C$ when ΔE is sufficiently fine. The power of the method resides in the fact that at a fixed value of E , multiple values of C are found simultaneously. If we do the opposite, fixing C , finding E , and then E must be determined one by one.
- (2) As $C \rightarrow \infty$, all eigenvalues approach zero, as they should. However, higher eigenvalues approach zero more slowly at larger values of C . Thus, when $v(r) \neq 0$, the C -scan will approach the eigenvalues of $v(r)$, with higher eigenvalues converging at larger values of C .
- (3) A single sweep in energy produces all the eigenvalues at the same time. An accuracy of 5–6 significant digits in determining E is easily achievable on a laptop computer.

We will now see the effectiveness of this method when applied to various potentials.

IV. HIDDEN SYMMETRIES IN THE COULOMB AND HARMONIC POTENTIALS

For the Coulomb potential $v_C(r) = -1/r$, the C -scan illustrating the convergence of the eigenvalues is shown in Fig. 2. We immediately notice something unusual. For large C , distinct higher energy levels corresponding to different

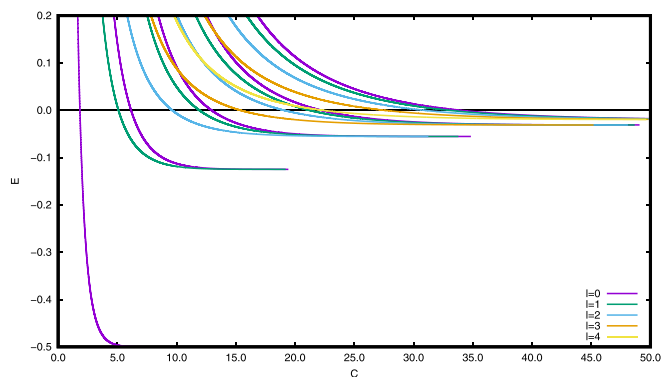


Fig. 2. The convergence of energy eigenvalues using the hardwall method for the three-dimensional Coulomb potential.

Table I. Calculated eigenvalues of the Coulomb potential. The first column lists the exact results $-1/(2n^2)$ with $n = \ell + n_r + 1$, from which n_r can be deduced for each state.

$-1/(2n^2)$	n	$\ell=0$	$\ell=1$	$\ell=2$	$\ell=3$	$\ell=4$
-0.50000	1	-0.49998
-0.12500	2	-0.12499	-0.12499
-0.05555	3	-0.05555	-0.05555	-0.05554
-0.03125	4	-0.03124	-0.03124	-0.03124	-0.03123	...
-0.02000	5	-0.01984	-0.01987	-0.01991	-0.01996	-0.01998

radial quantum numbers n_r and ℓ coalesce into a single level. Because the hardwall is spherically symmetric, its addition does not alter the spherical symmetry of the Coulomb potential. For spherical symmetry, each energy level with quantum number ℓ , regardless of n_r , is $2\ell + 1$ degenerate, meaning that all $2\ell + 1$ states with azimuthal quantum number $m = -\ell, \dots, -1, 0, 1, \dots, \ell$ have the same energy. However, as the hardwall is gradually removed in letting $C \rightarrow \infty$, further degeneracy is revealed, due to the hidden $SO(4)$ symmetry¹⁵ of the Coulomb potential.

The pattern of this degeneracy is also visible. The ground state $(\ell, n_r) = (0, 0)$ is nondegenerate. The next two states $(0, 1)$, $(1, 0)$ are degenerate. The next three states $(0, 2)$, $(1, 1)$, $(2, 0)$ are degenerate, with the energy depending only on the sum of ℓ and n_r as $E = -1/(2n^2)$, with $n = \ell + n_r + 1$. Thus, the hardwall method not only computes the eigenvalues but its C -scan also reveals the hidden symmetry and the pattern of degeneracy of the Coulomb potential. The resulting eigenvalues are shown in Table I.

For the harmonic potential $v_H(r) = (1/2)r^2$, the corresponding C -scan is shown in Fig. 3. Again, we observe energy degeneracy at large values of C and can therefore conclude that the three-dimensional harmonic oscillator also has a hidden symmetry (that of $SU(3)$).¹⁶

Let's see whether we can also deduce its pattern of degeneracy. There are two states $(\ell, n_r) = (0, 0)$, $(1, 0)$ that are nondegenerate. There are two states that are twofold degenerate: $[(0, 1), (2, 0)]$ and $[(1, 1), (3, 0)]$, threefold degenerate: $[(0, 2), (2, 1), (4, 0)]$ and $[(1, 2), (3, 1), (5, 0)]$, and fourfold degenerate. The degeneracy pattern is therefore for ℓ even, $[(0, 0)]$, $[(0, 1), (2, 0)]$, $[(0, 2), (2, 1), (4, 0)]$, $[(0, 3), (2, 2), (4, 1), (6, 0)]$, ... and for ℓ odd, $[(1, 0)]$, $[(1, 1), (3, 0)]$, $[(1, 2), (3, 1), (5, 0)]$, $[(1, 3), (3, 2), (5, 1), (7, 0)]$, ... (Degenerate levels are grouped together by square brackets.) Both the patterns of degeneracy can be accounted for if the energy depends only on $\ell + 2n_r$.

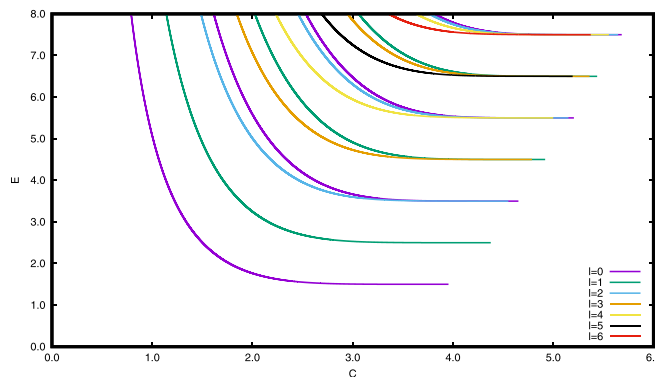


Fig. 3. The convergence of the energy eigenvalues for the three-dimensional harmonic potential.

Table II. Calculated eigenvalues of the harmonic potential. The first column is the exact result ($\ell + 2n_r + 3/2$).

$(\ell + 2n_r + 3/2)$	$\ell = 0$	$\ell = 1$	$\ell = 2$	$\ell = 3$	$\ell = 4$	$\ell = 5$	$\ell = 6$
1.50000	1.50002
2.50000	...	2.50001
3.50000	3.50001	...	3.50002
4.50000	...	4.50001	...	4.50002
5.50000	5.50001	...	5.50001	...	5.50001
6.50000	...	6.50001	...	6.50001	...	6.50002	...
7.50000	7.50001	...	7.50001	...	7.50001	...	7.50002

Therefore, we can deduce that the energy spectrum must be given by $\ell + 2n_r + 3/2$, where $3/2$ is the ground state energy of $(0, 0)$. This analytical result is compared to the computed spectrum given in Table II.

The hidden symmetry of the Coulomb and the harmonic potential is unique in each case. If we add the Coulomb and the harmonic potential, then the hidden symmetry is destroyed for the combined potential, as is illustrated in the C -scan of Fig. 4. We see that energy levels, which were k -fold degenerate in the harmonic oscillator case, now split into k energy levels for large C . The computed eigenvalues are shown in Table III. Because the Coulomb potential is strong only near the origin, it acts as a perturbation, and only modifies the low-lying spectrum of the harmonic oscillator.

V. WOODS-SAXON POTENTIAL

The Woods-Saxon potential^{9,17} describes the effective average force confining each nucleon in the interior of the nucleus as

$$V_{\text{WS}}(r) = \frac{u_0}{1+t} + \frac{u_1 t}{(1+t)^2}, \quad t = \exp\left[\frac{r-r_0}{a}\right], \quad (12)$$

where u_0 and u_1 fix the potential well depth, a is the surface thickness of the nucleus, and r_0 is the nuclear radius proportional to the mass number. We use the parameterization by Vanden Berghe *et al.*⁹ with $u_0 = -50$ MeV, $r_0 = 7$ fm, $a = 0.6$ fm, and $u_1 = -u_0/a$. We use the dimensionless form of the equation but restate the results in physical units for comparison. The convergence of the eigenvalues, with $\Delta r = 0.001$ and $\Delta E = 0.0005$, is shown in Fig. 5. Because the Woods-Saxon potential has no special symmetry, its C -scan shows close-by energy levels, but no degeneracy. A selected

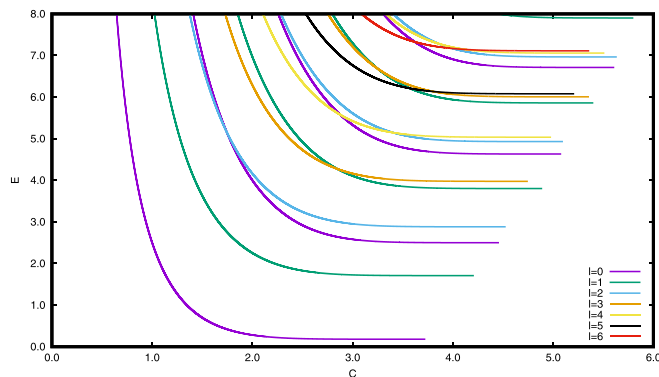


Fig. 4. The convergence of energy eigenvalues for the Coulomb plus harmonic potential.

Table III. Calculated eigenvalues of the Coulomb plus harmonic potential. There is now no degeneracy.

n_r	$\ell = 0$	$\ell = 1$	$\ell = 2$	$\ell = 3$	$\ell = 4$	$\ell = 5$	$\ell = 6$
0	0.17968
1	...	1.70903
2	2.50001	...	2.88224
3	...	3.80193	...	3.97553
4	4.63196	...	4.93068	...	5.03608
5	...	5.86036	...	6.00654	...	6.07947	...
6	6.71260	...	6.96584	...	7.05815	...	7.11255

set of 21 converged eigenvalues are compared with exact results in Table IV. Our eigenvalues agree with published results up to five significant digits.

VI. SOLVING ONE DIMENSIONAL PROBLEMS

By setting $\ell = 0$, the hardwall method can also solve strictly one-dimensional problems. The condition $u(0) = 0$ can be interpreted as having a real, infinite barrier at $x = 0$. In this case, an interesting problem for students to explore is the “bouncing ball” problem described by

$$-\frac{\hbar^2}{2m} \frac{d^2 u}{dx^2} + mgxu(x) = Eu(x). \quad (13)$$

This case is a trivial classical mechanics problem, where a ball of mass m is dropped from a given height h with energy mgh . Assuming that there is no friction and the floor is perfectly elastic, the ball will bounce forever in this “bound state,” returning again and again to its original height. This behavior is to be contrasted with the complexity of the quantum mechanical solution described in the following and rarely discussed in textbooks.

Following our dimensionless reduction procedure we have described, by choosing the length $a = (\hbar^2/m^2g)^{1/3}$ and the unit of energy $E_0 = \hbar^2/(ma^2)$, Eq. (13) takes the dimensionless form

$$\frac{d^2 u}{dx^2} = 2(x - E)u, \quad (14)$$

identical to Eq. (7) with $\ell = 0$. To determine the set of eigenvalues, we change the independent variable to $s = 2^{1/3}(x - E)$, so that Eq. (14) becomes

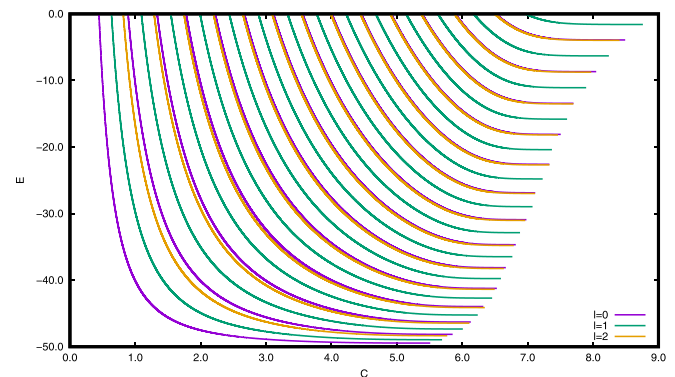


Fig. 5. The convergence of energy eigenvalues using the hardwall method for the Woods-Saxon potential as parameterized in Ref. 9.

Table IV. Comparison of calculated eigenvalues to published values (Ref. 9) for the Woods-Saxon potential for angular momentum channels $\ell = 0, 1, 2$. Only these even n_r state energies are given in Table 2 of Ref. 9. The unit of energy is MeV.

n_r	Exact results			Calculated results		
	$\ell = 0$	$\ell = 1$	$\ell = 2$	$\ell = 0$	$\ell = 1$	$\ell = 2$
0	-49.457788728	-48.951731623	-48.34981052	-49.4570	-48.9510	-48.3485
2	-46.290753954	-45.237176986	-44.121537377	-46.2905	-45.2370	-44.1215
4	-41.232607772	-39.767208069	-38.253426539	-41.2325	-39.7670	-38.2530
6	-34.672313205	-32.868392986	-31.026820921	-34.6720	-32.8680	-31.0265
8	-26.873448916	-24.794185466	-22.689041510	-26.8730	-24.7940	-22.6890
10	-18.094688282	-15.812724871	-13.522303352	-18.0945	-15.8125	-13.5220
12	-8.676081670	-6.308097192	-3.972491432	-8.6760	-6.3080	-3.9720

$$\frac{d^2 u}{ds^2} = su. \quad (15)$$

The solution of Eq. (15) is the Airy function $u(x) = Ai(2^{1/3}(x - E))$. The requirement that $u(0) = 0$ gives the eigenvalue condition

$$Ai(-2^{1/3}E) = 0. \quad (16)$$

Because the negative zeros of the Airy function are widely available: 2.33811, 4.08795, 5.52056, ..., the energy levels of our bouncing ball are 1.85576, 3.24461, 4.38167, Running the hardwall method with Eq. (14) will immediately yield these values without any reference to the Airy function.

This result means that the quantum ball can bounce only from a height of 1.85576a, 3.24461a, 4.38167a, The height is *quantized*! An interesting discussion question for students is how will the quantum ball bounce if it were released not at these heights? Also interesting is to determine a and E_0 for an electron using earth's gravity constant g . For further details on this problem, see Ref. 18.

For a symmetric one-dimensional potential, the condition $u(0) = 0$ picks out all the odd state energies. We will leave it to interested readers to determine what the correct boundary condition is for obtaining the even state energies. For the left-right symmetric potential $V(x) = |x|$, we will simply assert that the first two even state energies are 0.8086 and 2.5781, and for the harmonic oscillator potential $V(x) = x^2/2$, the energy eigenvalues are the familiar values $n + 1/2$ for n even.

VII. CONCLUSION

We have demonstrated a simple method of solving the radial Schrödinger equation by trying all eigenvalues systematically, up to a certain precision. The hardwall method relies on the insight that any trial eigenvalue E is an exact eigenvalue for a given potential plus a hardwall at some radius C . By plotting E versus C , the eigenvalues can be determined to five or more significant digits for large C . Moreover, this C -scan of the spectrum can detect hidden symmetries by revealing additional degenerate energy levels beyond spherical symmetry and their patterns of degeneracy. The method is a valuable tool, not just for solving the radial Schrödinger equation, but also for teaching the emergence of accidental degeneracies from hidden symmetries.

The method can also be applied to a strictly one-dimensional Schrödinger equation, with interesting applications to the bouncing ball problem. We leave it to readers to devise the correct boundary condition for obtaining the even state energies for a left-right symmetric potential.

ACKNOWLEDGMENTS

The authors thank Rory O'Dwyer for help in solving for the even state energies of a symmetric 1D potential.

^aElectronic mail: chin@physics.tamu.edu

^bElectronic mail: john.massey@tamu.edu

¹J. S. Bolemon, "Computer solutions to a realistic one-dimensional Schrödinger equation," *Am. J. Phys.* **40**, 1511–1517 (1972).

²S. E. Koonin and D. C. Meredith, *Computational Physics-Fortran Version* (Taylor and Francis, London, 1990).

³P. L. DeVries, *A First Course in Computational Physics* (John Wiley & Sons, New York, 1994).

⁴F. J. Vesely, *Computational Physics-An Introduction* (Plenum Press, New York, 1994).

⁵N. J. Giordano, *Computational Physics* (Prentice-Hall, New Jersey, 1997).

⁶H. Gould, J. Tobochnik, and W. Christian, *An Introduction to Computer Simulation Methods*, 3rd ed. (Pearson Addison-Wesley, San Francisco, 2007).

⁷R. H. Landau, M. J. Paez, and C. C. Bordeianu, *A Survey of Computational Physics* (Princeton U. P., Princeton, NJ, 2008).

⁸L. Gr. Ixaru and M. Rizea, "Comparison of some four-step methods for the numerical solution of the Schrödinger equation," *Comput. Phys. Commun.* **38**, 329–337 (1985).

⁹G. Vanden Berghe, V. Fack, and H. E. De Meyer, "Numerical methods for solving radial Schrödinger equations," *J. Comput. Appl. Math.* **28**, 391–401 (1989).

¹⁰S. A. Chin and P. Anisimov, "Gradient symplectic algorithms for solving the radial Schrödinger equation," *J. Chem. Phys.* **124**, 054106 (2006).

¹¹B. A. Jugdutt and F. Marsiglio, "Solving for three-dimensional central potentials using numerical matrix methods," *Am. J. Phys.* **81**, 343–350 (2013).

¹²B. Numerov, "A method of extrapolation of perturbations," *Royal Astronomical Society* **84**, 592–601 (1924).

¹³P. C. Chow, "Computer solutions to the Schrödinger equation," *Am. J. Phys.* **40**, 730–734 (1972).

¹⁴D. R. Hartree, *The Calculation of Atomic Structures* (Pergamon Press, London, 1957).

¹⁵G. Baym, *Lectures on Quantum Mechanics* (W.A. Benjamin, New York, 1969).

¹⁶D. M. Fradkin, "Three-dimensional isotropic harmonic oscillator and SU₃," *Am. J. Phys.* **33**, 207–211 (1965).

¹⁷R. D. Woods and D. S. Saxon, "Diffuse surface optical model for nucleon-nuclei scattering," *Phys. Rev.* **95**, 577–578 (1954).

¹⁸S. Flügge, *Practical Quantum Mechanics* (Springer-Verlag, Berlin, 1971).